Materials Sciences and Application, 2011, 2, 827-833
doi:10.4236/msa.2011.27112 Published Online July 2011 (http://www.SciRP.org/journal/msa)

Interaction of 8 MeV Electron Beam with P31 *Bombyx mori* Silk Fibers

Sangappa Halabhavi[1*], Sangappa Asha[1], Puttanna Parameswar[2], Rudrappa Somashekar[2], Sanjeev Ganesh[3]

[1]Department of Studies in Physics, Mangalore University, Mangalagangotri, India; [2]Department of Studies in Physics, University of Mysore, Mysore, India; [3]Microtron Center, Mangalore University, Mangalagangotri, India.
Email: syhalabhavi@yahoo.co.in

Received December 2nd, 2010; revised March 21st, 2011; accepted May 21st, 2011.

ABSTRACT

The 8 MeV electron radiation-induced changes in physical and thermal properties in P31 (Bombyx mori) silk fibers were investigated and has been correlated with the applied radiation doses. Irradiation of fiber samples were carried out in dry air at room temperature using an electron beam accelerator for varied radiation doses in the range of 0 - 100 kGy. Physical properties of the irradiated silk fibers were studied using XRD, FT-IR and thermogravimetric analysis (TGA) and compared with unirradiated fiber sample. Interesting results are discussed in this report.

Keywords: *Fiber*, *Irradiation*, *Physical*, *Thermal Properties*

1. Introduction

For several centuries, silk of Bomyx mori has been used as a textile fiber [1] and there is rigorgitated research in recent times to produce application oriented silk fibers. These changes can be brought about by genetically modifying the cocoons or by induced modification brought about with the high energetic particle interaction with silk fibers. These changes are quantified interms of microstructural parameters of silk fibers. These parameters and their magnitude influence the property and strength of the fibers. Such studies have not been carried out except for the chemical effects on these fibers [2-7]. Okuyama's group [8] have reported crystal structure for silk-I and silk-II fibers. Somashekar's group [9,10] have reported the effect of degumming and dye processing on the microstructural parameters in pure Mysore silk, nistari, NB7 and NB18 silk fibers. Sangappa *et al.* have studied microstructural parameters in nistari, Cnichi, Hosa Mysore and pure Mysore silk fibers [11,12]. Takeshita and group [13] have studied the effect of electron beam irradiation on silk fibers. Effects of gamma irradiation on biodegradation of *Bombyx mori* silk fibers have been carried out by Kojthung's group [14]. Recently we have reported the changes in polymers like HPMC due to irradiation.

At the microscopic level, the polymer degradation is characterized by macromolecular chain splitting, creation of low mass fragments, production of free radicals, oxidation and cross-linking. These effects the macroscopic properties like mechanical strength, color, electrical conductivity and so on [15]. The resulting change in the properties of the polymer may extend the range of applications for the material [16]. The study of the microstructural parameters, chemical and thermal properties are of great importance, especially when the polymer properties are being modified by ionizing radiation. In this paper we have investigated the microstructuralline changes (physical), structural changes and thermal stability of the P31 Bombyx mori silk fiber by X-ray diffraction study (WAXS), FT-IR spectra analysis and thermogravimetric (TGA) analysis after electron beam (EB) irradiation.

2. Experimental

2.1. Sample Preparation

For our study we have used raw P31 silk fiber belonging to *Bombyx mori* family which comes under the classification Multivoltine on the basis of shape, color, denier and life cycle of the fibers/cocoons. Cocoons were collected from the germ plasma stock of the Department of Sericulture, University of Mysore India, which were then cooked in boiling water (100˚C) for 2 min. to soften the sericin and transferred to water bath at 65˚C for 2 min. Then the cocoons were reeled in warm water with the

help of mono cocoon reeling equipment EPPROUVITE. The characteristic features of these fibers are that they are white in color with an average filament length of 350 meter and denier being in the range 1.8 - 2.0. These fibers were mounted on rectangular frame in *just taut* condition which does not involve any mechanical stretching of fibers. The whole process, starting from reeling to mounting of fibers, does not involve any type of mechanical deformation.

2.2. Electron Beam Irradiation

Irradiation of P31 silk fibers were done at Microtron Center, Mangalore University using the electron beams (by lanthanum hexa fluorite source). The monochromatic beam is made to fall on samples kept at particular distance and the following beam features given in **Table 1**. The dose delivered to different samples is measured by keeping alanine dosimeter with sample during irradiation. The samples were subjected to various integral doses, which were accumulated in steps, where the irradiation doses were conducted at 0, 25, 50, 75 and 100 kGy.

2.3. Polymer Characterization

P31 *Bombyx mori* silk fibers (raw) and 8 MeV electrons beam irradiated were characterized by different techniques such as X-ray diffraction (XRD), Fourier transforms IR (FT-IR) spectroscopy and thermal technique, like thermogravimetric analysis (TGA) was used.

2.3.1. X-Ray Diffraction Measurements

The XRD diffractograms of the fiber samples were recorded using a Rigaku Miniflex-II X-ray diffractometer with Ni filtered, CuKα radiation of wavelength λ = 1.5406 Å, with a graphite monochromator. The scattered beam was focused on a detector. The specifications used for the recordings were 40 kV, 30 mA. The samples were scanned in the 2θ range 10˚ - 50˚ with a scanning speed and step size of 1˚/min and 0.01˚ respectively and diffraction scans are given in **Figure 1**.

Table 1. Specifications of the electron beam accelerator and irradiation conditions.

1. Beam energy	8 MeV
2. Beam current	20 mA
3. Pulse repetition rate	50 Hz
4. Pulse width	2.2 μs
5. Distance source to sample	30 cm
6. Time of exposure	25 min
7. Dose range	0 - 100 kGy
8. Atmosphere	air
9. Temperature	24˚C

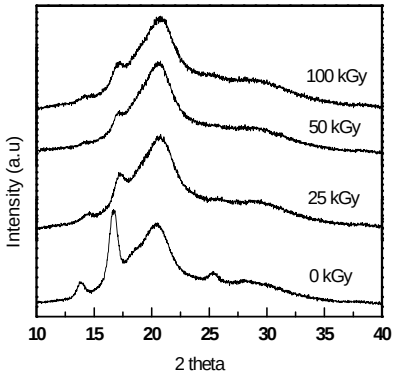

Figure 1. XRD scans of pure and 8 MeV electron irradiated polymer samples.

2.3.2. FT-IR spectra

Fourier transform infrared (FT-IR) spectra of the virgin and 8 MeV EB irradiated P31 *Bombyx mori* silk fiber samples was recorded in transmission mode Thermo Nicolet, Avatar 370, FTIR spectrophotometer having a resolution 4 cm^{-1} in the wave number range 500 - 4000 cm^{-1}.

2.3.3. Thermogravimetric Spectra

The samples were weighed in microbalance and crimped in aluminum pans. Thermogravimetric analysis (TGA) of these samples was done by Perkin Elmer Thermal Analysis system with nitrogen as flushing gas. The temperature range scanned was 25˚C - 800˚C at a predetermined rate of 10˚C/min. The thermogram, *i.e.*, a plot of weight percent as a function of temperature, was used to study the variation in the thermal stability of the polymer. Samples of 1.565 - 7.623 mg were used for the measurement.

3. Theory

Microstructural parameters such as crystal size (⟨N⟩) and lattice strain (g in %) are usually determined by employing Fourier method of Warren and Averbach [17], and Warren [18]. The intensity of a profile in the direction joining the origin to the center of the reflection can be expanded in terms of Fourier cosine series:

$$I(s)=\sum_{n=-\infty}^{\infty} A(n)\cos\{2\pi nd\,(s-s_o)\} \qquad (1)$$

where the coefficients of the harmonics $A(n)$ are functions of the size of the crystallite and the disorder of the lattice. Here, s is sin (θ)/(λ), s_o being the value of s at the peak of a profile, n is the harmonic order of coefficient, and d is the lattice spacing. The Fourier coefficients can be expressed as:

$$A(n) = A_s(n)\; A_d(n) \qquad (2)$$

For a paracrystalline material, $A_d(n)$ can be obtained, with Gaussian strain distribution [19],

$$A_d(n) = \exp\left(-2\pi^2 m^2 n\, g^2\right) \qquad (3)$$

where "m" is the order of the reflection and g = (Δd/d) is the lattice strain. Normally one also defines mean square strain $\langle \varepsilon^2 \rangle$, which is given by g^2/n. This mean square strain is dependent on n, whereas not g [20,21]. For a probability distribution of column lengths $P(i)$, we have:

$$A_s(n) = 1 - \frac{nd}{D} - \frac{d}{D}\left[\int_0^n iP(n)di - n\int_0^n P(i)di\right] \quad (4)$$

where $D = \langle N \rangle d_{hkl}$ is the crystallite size and "i" is the number of unit cells in a column. In the presence of two order of reflections from the same set of Bragg planes, Warren and Averbach [17,18] have shown a method of obtaining the crystal size ($\langle N \rangle$) and lattice strain (g in %). But in polymer it is very rare to find multiple reflections. So, to determine the finer details of microstructure, we approximate the size profile by simple analytical function for $P(i)$ by considering only the asymmetric functions. Another advantage of this method is that the distribution function differs along different directions. Whereas, a single size distribution function that is used for the whole pattern fitting, which we feel, may be inadequate to describe polymer diffraction patterns [20-22]. Here it is emphasized that the Fourier method of profile analysis (single order method used hare) is quite reliable one as per the recent survey and results of round Robin test conducted by IUCr [23]. In fact, for refinement, we have also considered the effect of back-ground by introducing a parameter [see for details regarding the effect of back-ground on the microcrystalline parameters]. For the sake of completeness, we reproduce the following equations which are used in the computation of microstructural parameters.

The Exponential Distribution

It is assumed that there are no columns containing fewer than p unit cells and those with more decay exponentially. Thus, we have [24],

$$P(i) = \{ 0 \text{ ; if } p < i \ \{\alpha \exp\{-\alpha(i-p)\} \text{ ; if } p \geq i \quad (5)$$

where $\alpha = 1/(N - p)$ Substituting this in Equation (4), we get:

$$A_s(n) = \{ A(0)\,(1 - n / \langle N \rangle) \text{ ; if } n \leq p \ \{A(0)\ \{\exp[-\alpha(n - p)]\} / (\alpha N); \text{ if } n \geq p \quad (6)$$

where α is the width of the distribution function, "i" is the number of unit cells in a column, n is the harmonic number, p is the smallest number of unit cells in a column and ⟨N⟩, the number of unit cells counted in a direction perpendicular to the (hkl) Bragg plane.

4. Results and Discussion

4.1. X-Ray Profile Analysis Study

Figures 2(a-d) show the comparison between simulated and experimental profiles for 8 MeV electron irradiated and pure fiber sample for Bragg's (110) reflection. The simulated profile was obtained with the using appropriate model parameters. This procedure was followed for all the other treated samples at different radiation doses. The computed microcrystalline parameters such as crystallite size <*N*>(*number of unit cells*), lattice strain *g* in %, the width of the crystallite size distribution (α) and the standard deviation are given in **Table 2**.

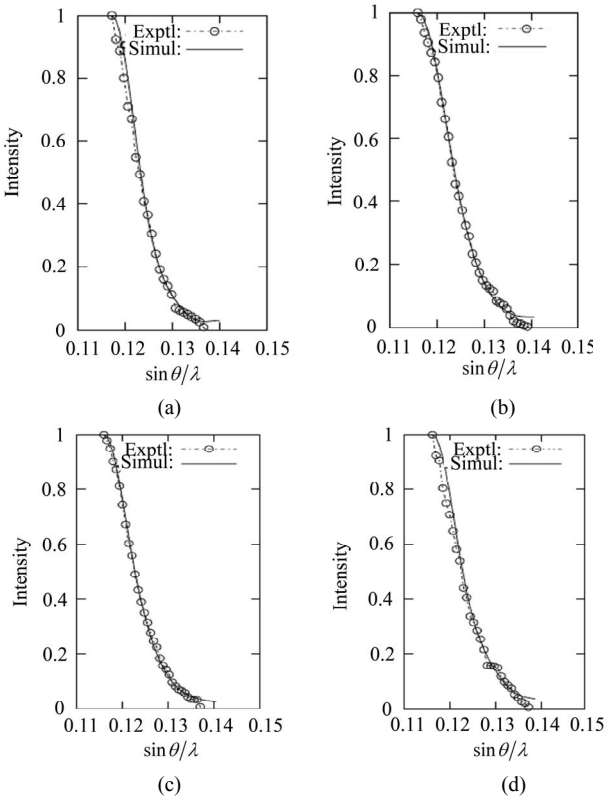

Figure 2. (a-d) Experimental and simulated intensity profiles of X-ray reflection of Silk fiber samples obtained with Exponential column length distribution function.

For the pure sample the surface weighted crystallite size is 30.30 Å, in the case of 25 kGy irradiated fiber sample it is 27.13 Å, in 50 kGy EB irradiated fiber sample surface weighted crystallite size is 29.56 Å, and in the case of 100 kGy the size is 30.88 Å. When the polymer is subjected to the ionizing radiation like EB irradiation mainly two processes occurs, 1) Chain scissioning 2) Cross-linking. Initially these two processes simultaneously occur at lower doses and later the cross-linking dominates. From the wide angle X-ray scattering (WAXS) study of electron irradiated P31 silk fiber (*Bombyx mori*) samples, we have observed a significant change in the values of microstructural parameters changes after high energy electron irradiation. This causes the cross-linking of small polymer units leading to

Table 2. Microstructural parameters of Electron irradiated polymer samples computed by Exponential distribution function.

Sample	<*N*>	*g* in %	α*	D_s (Å)	delta
0 kGy	7.01 ± 0.34	0.5 ± 0.02	0.013	30.35	0.049
25 kGy	7.01 ± 0.34	0.5 ± 0.02	0.012	27.13	0.042
50 kGy	6.90 ± 0.34	0.5 ± 0.02	0.013	29.56	0.049
100kGy	7.11 ± 0.43	0.1 ± 0.01	0.003	30.88	0.061

the formation of a rigid 3-dimensional network. Increasing crystallite size with increasing irradiation dose shows that there is an increase in sample tensile strength of the fiber [25]. This aspect suggests that for 100 kGy integral dose irradiated fiber, there is an increase in formation of cross-linking bonds between inter polymer chains than unirradiated one. Also, it essentially implies, the efficiency of cross-linking in these fibers is improved to a large extent by means of electron irradiation. We have observed that the lattice strain and its variation for various values of the radiation doses (kGy) in polymer samples are very small and this may be due to inherent model dependent factor.

4.2. FT-IR Spectral Analysis

The FT-IR absorbance spectra for the virgin and the 8 MeV electron irradiated P31 *Bombyx mori* silk fiber samples are shown in **Figures 3(a-c)**. Silk fibroin conformation was often investigated using FT-IR spectroscopy since the FT-IR spectrum represents typical absorption bands sensitive to the molecular conformation. The FT-IR spectrum of pure silk fiber showed strong absorption bands of amide-I, which is useful for the analysis of the secondary structure of proteins and is mainly related with the C=O stretching, and it occurs in the range of 1700 - 1750 cm^{-1}(**Figure 3(a)**). Amide-II, which falls in 1450 - 1480 cm^{-1} range, is related with the N-H bonding and C-H stretching vibration. Amide-III occurs in the range of 1160 - 1210 cm^{-1} and it results from in phase combinations of C-N stretching and C=O bending vibration [26]. 50 kGy irradiated fiber sample shows some absorption bands. Characteristics absorption bands assigned to the peptide bonds (-CONH-) that originates known as amide-I amide-II and amide-III which are not observed in the higher dose (100 kGy) electron irradiated samples. With an increasing the irradiation dosage there are no characteristic absorption bands when comparing the pure and lower dose irradiated samples. This may be due to cross linking of the fiber. This is also supported by XRD and TGA analysis.

4.3. Thermogravimetric Analysis Study

The thermograms obtained for the raw and the irradiated P31 silk fibers are shown in **Figure 4**. The thermograms of both the raw and 8 MeV electrons irradiated P31 silk fiber showed three distinct regions. For the virgin silk fiber first region, starting from room temperature up to 218˚C the weight loss is due to water vaporization (drying). The weight change was not significant and the sample was thermally stable. In the second, rather narrow region from 218˚C to 398˚C the fiber experienced a great weight loss, because of the thermal decomposition. About 65% of the sample decomposed into volatiles. After 398˚C the fiber was slowly decomposed and about 90 of the sample decomposed into volatiles [27]. In the case of electron beam irradiated fiber the thermograms showed into three distinct regions. In the 50 kGy EB irradiated P31 silk fiber, the first region, starting from room temperature up to 237˚C the weight loss is due to water vaporization. The weight change is not significant and the irradiated fiber is thermally stable. In the second region from 237˚C to 419˚C, the fiber experienced a great weight loss because of the thermal decomposition. About 60% of the sample decomposed into volatiles. At 600˚C about 74% decomposed and at 800˚C about 80% decomposed.

In the 100 kGy dose irradiated fiber sample also showed the three regions and at 400˚C, about 54% of the sample decomposed. At 600˚C about 66.5% decomposed, at 800˚C about 70% (**Table 3**) decomposed into volatiles. From this study it is clear that as the irradiation dose increases the cross-linking of the polymer increases and thermal stability of the irradiated samples increases. The weight loss decreases as irradiation dose increases.

5. Conclusions

From the wide angle X-ray scattering (WAXS) study of electron irradiated P31 silk fiber (*Bombyx mori*) samples, we have observed a significant change in the values of micro structural parameters occurs. This is because of the cross-linking of small polymer units leading to the formation of a rigid 3-dimensional network. FT-IR study of 8MeV electron irradiated polymer fibers undergoes structural modifications.

From the TGA thermograms, we noticed the following: 1) an increasing irradiation dose resulted in an increase in the thermal stability of silk fibers. 2) For all the investigated samples, there was almost 10% - 15% weight loss due to water vaporization and decomposition temperature increases with increasing dose, this is because of the

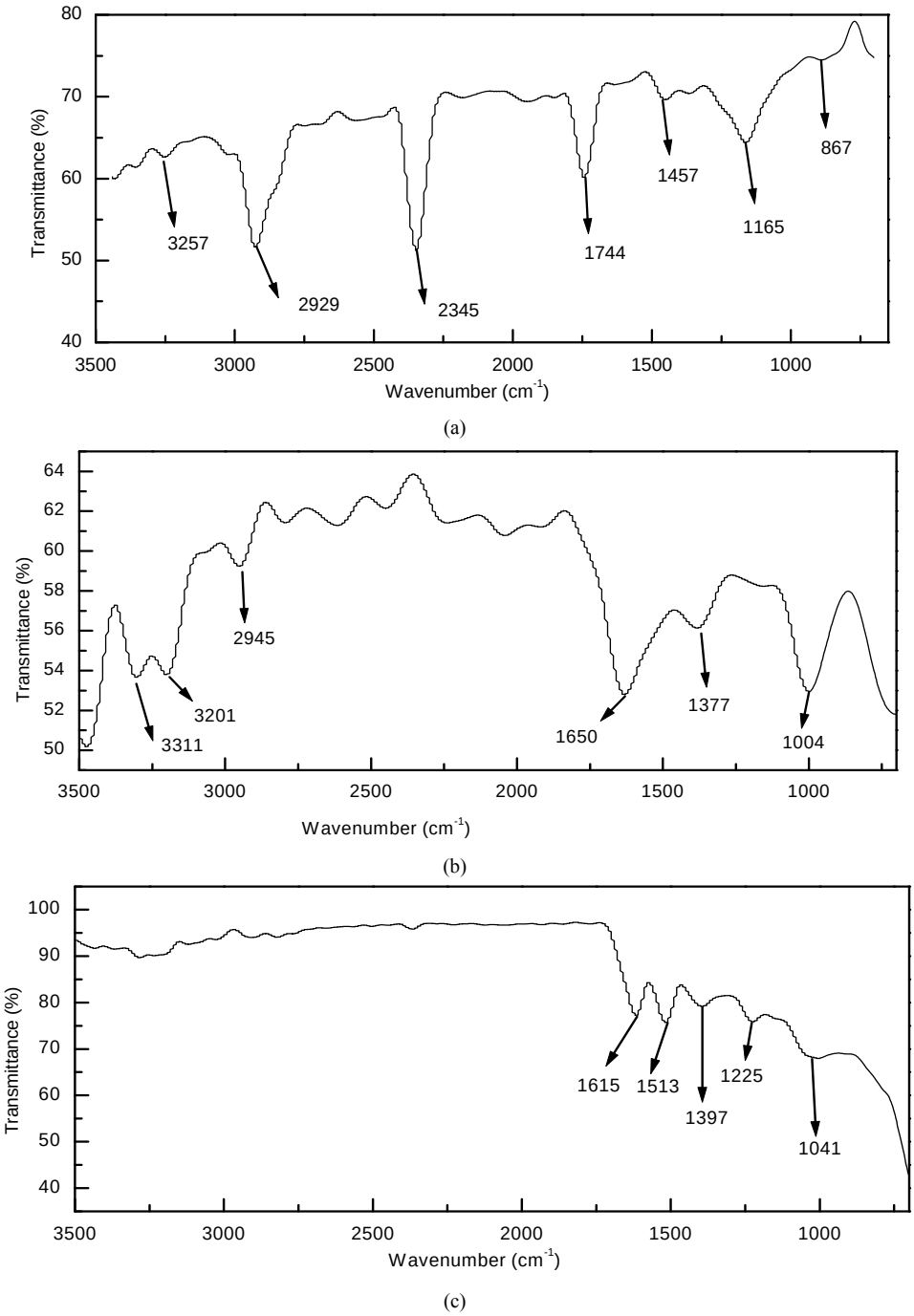

Figure 3. FT-IR spectra's (a) virgin (b) 50 kGy (c) 100 kGy EB irradiated samples.

Table 3. Temperature of decomposition at different weight loss (%) of P31 Silk fiber before and after EB irradiation.

Irradiation Dose (kGy)	Temperature (˚C)							
	100	200	300	400	500	600	700	800
0	10.45	10.77	32.07	62.64	72.96	77.75	82.75	87.39
50	09.39	10.24	28.55	61.24	68.91	74.24	77.75	80.09
100	07.79	08.64	26.42	54.64	68.91	66.25	68.91	69.98

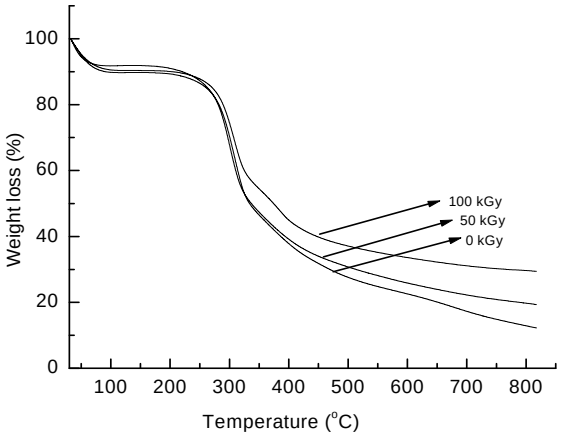

Figure 4. TGA thermograms of (a) virgin (b) 50 kGy (c) 100 kGy EB irradiated samples.

cross-linking of P31 silk fiber due to EB irradiation.

6. Acknowledgements

The authors are thankful to University Grant Commission, New Delhi, Govt of India, for providing financial assistance through a project F. No. 33-14/2007 (SR). The authors are also thankful to STIC Cochin University for extending the experimental facilities.

REFERENCES

[1] D. Lance Miller, S. Putthanarat and W. W. Adoms, "Investigation of the Nano Fibrillar Morphology in Silk Fiber by Small Angle X-Ray Scattering and Atomic Force Microscopy," *International Journal of Biological Macromolecules*, Vol. 24, No. 2, March 1999, pp. 159-165. doi:10.1016/S0141-8130(99)00024-0

[2] N. Mohanthy, H. K. Das, P. Mohanthy and E. Mohanthy, "Modification of Muga Silk by Methyl-Methacrylate.II," *Journal of Macromolecular Science*, Vol. 32, 1995, pp. 1103-1108. doi:10.1080/10601329508019151

[3] Y. Kavahara, M. Shioya and A. Takaku, "Influence of Swelling of Non-Crystalline Regions in Silk Fibers on Modification with Methacrylamide," *Journal of Applied Polymer Science*, Vol. 59, 1996, pp. 51-56. doi:10.1002/(SICI)1097-4628(19960103)59:1<51::AID-APP8>3.0.CO;2-L

[4] G. Freddi, M. R. Massafra, S. Beretta, S. Shibata, Y. Gotch, H. Yasui and M. T.Sukuda, "Structure and Properties of Bombyx Mori Silk Fibers Grafted with Methacrylamide (MAA) and 2-Hydroxy Ethylmethacrylate (HEMA)," *Journal of Applied Polymer Science*, Vol. 60, 11, 1996, pp.1867-1876. doi:10.1002/(SICI)1097-4628(19960613)60:11<1867::AID-APP10>3.0.CO;2-Z

[5] M. Tsukuda, M. Obo, H. Kato, G. Freddi and F. Zenetti, "structure and Dyeability of Bombyxmori Silk Fibers with Different Filament Sizes," *Journal of Applied Polymer Science*, Vol. 60, No. 10, 1996, pp. 1619-1627. doi:10.1002/(SICI)1097-4628(19960606)60:10<1619::AID-APP14>3.0.CO;2-#

[6] M. Tsukuda, Y. Gotch, M. Nagura, N. Minoura, N. Kasai and G. Freddi, "Structural Changes of Silk Fibroin Membrance Induced by Immersion in Methanol Aqueous Solution," *Journal of Polymer Science* (*B*), Vol. 32, 1994, pp. 961-968. doi:10.1002/polb.1994.090320519

[7] H. Somashekarappa, N. Selvakumar, V. Subramaniam and R. Somashekar, "Structure-Property Relation in Varieties of Acid Dye Processed Silk Fibers," *Journal of Applied Polymer Science*, Vol. 59, 1996, pp. 1677-1683. doi:10.1002/(SICI)1097-4628(19960314)59:11<1677::AID-APP3>3.0.CO;2-L

[8] K. Okuyama, K. Takanashi, Y. Nakajima, Y. Hasegawa, K. Hirabayashi and N. Nishi, "Analysis of Silk I Structure by X-Ray and Electron Diffraction Method," *Journal of Service Science*, Vol. 57, 1988, pp. 23-30.

[9] H. Somashekarappa, V. Annadurai, Sangappa, G. Subramanya and R. Somashekar, "Structure-Property Relation in Varities of Acid Dye Processed Silk Fibers," *Materials Letters*, Vol. 53, No. 6, 2002, pp. 415-420. doi:10.1016/S0167-577X(01)00517-1

[10] H. Somashekarappa, G. S. Nadgir, T. H. Somashekar, J. Prabhu and R. Somashekar, "WAXS Studies on Silk Fibers Treated with Acid (Blue) and Metal Complex (Brown) Dyes," *Polymer*, Vol. 39, No. 1, 1998, pp. 209-213. doi:10.1016/S0032-3861(97)00220-6

[11] Sangappa, K. Okuyama and R. Somashekar, "Stain –Tensor Components, Crystallite Shape and Their Effects on Crystalline Structure in Silk I," *Journal of Applied Polymer Science*, Vol. 91, 2004, pp. 3045-3058.

[12] Sangappa, S. S. Mahesh and R. Somashekar, "Crystal Structure of Raw Pure Mysore Silk Fiber Based on (Ala-Gly) 2–Ser–Gly Peptide Sequence Using Linked-Atom-Least-Squares method," *Journal of Bioscience*, Vol. 30, No. 2, 2005, pp. 259-268. doi:10.1007/BF02703707

[13] H. Takeshita, K. Ishida, Y. Kamiishi, F. Yoshii and T. Kume, "Production of Fine Powder from Silk by Radiation," *Macromolecular Materials and Engineering*, Vol. 283, 2000, pp.126-131. doi:10.1002/1439-2054(20001101)283:1<126::AID-MAME126>3.0.CO;2-#

[14] A. Kojthung, P. Meesilpa, B. Sudatis, L. Treeratanapiboon, R. Udomsangpetch and B. Oonkhanond, "Effects of Gamma Irradiation on Biodegradation of Bombyx Mori Silk Fibroin," *International Biodeterioration and Biodegradation*, Vol. 62, No. 4, 2008, pp. 487-490. doi:10.1016/j.ibiod.2007.12.012

[15] G. Wang, G. Pan, L. Dow, S. Jiang and Q. Dai, "Proton Beam Modification of Isotactic Polypropylene," *Nuclear Instruments and Methods in Physics Research Section B*, Vol. 27, No. 3, 1987, pp. 410-416. doi:10.1016/0168-583X(87)90521-0

[16] Sangappa, S. Asha, T. Demappa, Ganesh Sanjeev, P. Parameswara and R. Somashekar, "Spectroscopic and Thermal Studies of 8 MeV Electron Beam Irradiated HPMC Films," *Nuclear Instruments and Methods in*

Physics Research Section B, Vol. 267, No. 14, 2009, pp. 2385-2389. doi:10.1016/j.nimb.2009.04.007

[17] B. E. Warren and B. L. Averbach, "Introduction to the Riveted Method," *Journal of Applied Physics*, Vol. 21, 1950, pp. 595-599. doi:10.1063/1.1699713

[18] B. E. Warren, "A Generalized Treatment of Cold Work in Powder Patterns," *Acta Crystallographica*, Vol. 8, 1955, pp. 483-486. doi:10.1107/S0365110X55001503

[19] I. H. Hall and R. Somashekar, "The Determination of Crystal Size and Disorder from the X-Ray Diffraction Photograph of Polymer Fiber 2. Modelling Intensity Profiles," *Journal of Applied Crystallography*, Vol. 24, 1991, pp. 1051-1059. doi:10.1107/S0021889891007707

[20] R. Ribarik, T. Ungar, J. Gubicza, "MWP-Fit: A Program for Multiple Whole-Profiles Fitting of Diffraction Peak Profiles by Ab Initio Theoretical Functions," *Journal of Applied Crystallography*, Vol. 34, 2001, pp. 669-676. doi:10.1107/S0021889801011451

[21] N. C. Popa, D. Balzar, "An Analytical Approximation for a Size-Broadened Profile Given by the Lognormal and Gamma Distributions," *Journal of Applied Crystallography*, Vol. 35, 1995, pp. 338-346. doi:10.1107/S0021889802004156

[22] P. Scardi and M. Leoni, "Continuous Hydrothermal Synthesis of Inorganic Materials in a System," *Acta Crystallographica Section A*, Vol. 57, 2001, pp. 604-613. doi:10.1107/S0108767301008881

[23] D. Balzar, "Report on the Size-Strain Round Robin," *IUCr News Letter*, Vol. 228, 2002, p. 14

[24] R. Somashekar, H. Somashekarappa, "X-Ray Diffraction-Line BroadeningAnalysis: Paracrystalline Method," *Journal of Applied Crystallographica*, Vol. 130, 1997, pp. 147-152. doi:10.1107/S0021889896010023

[25] M. Uenoyama, S. Shukushima, H. Hayami and S. Nishimoto, "Development of Radiation Cross-Linked Polypropylene," *SEI Technical Review*, Vol. 54, 2002, pp. 61-66.

[26] A. Vasconcelos, G. Freddi and A. Cavaco-Paulo, "Bio Degredible Materials Based on Silk Fibroin and Keratin," *Biomacromolecules*, Vol. 9, No. 4, 2008, pp. 1299-1305. doi:10.1021/bm7012789

[27] M. Srisa-Ard, Y. Baimark and Y. Srisuwan, "Conformation Transition and Thermal Properties Study of Silk Fibroin and Poly(∈-Caprolactone) Blend," *Journal of Applied Science*, Vol. 8, No. 19, 2008, pp. 3518-3523.

